Journal of Robotics and Control (JRC)
Volume 6, Issue 3, 2025
ISSN: 2715-5072, DOI: 10.18196/jrc.v6i3.26211

Sensorless Hybrid Control System for Boost Converter in Presence of Uncertain Dynamics

Ibrahim K. Mohammed [1*], Hajar K. Ibrahim [2], Salih M. Attya [3], Damian Giaouris [4]
[1] Systems and Control Engineering Department, College of Electronics Engineering, Ninevah University, Mosul, Iraq
[2] Electronic Engineering Department, College of Electronics Engineering, Ninevah University, Mosul, Iraq
[3] Computer Science Department, College of Education, Al-Noor University, Mosul, Iraq
[4] Electrical and Electronic Engineering Department, School of Engineering, Newcastle University, Newcastle Upon Tyne, England
Email: [1] ibrahim.mohammed@uoninevah.edu.iq, [2] hajar.khaleel@uoninevah.edu.iq, [3] salih.mahmoud@alnoor.edu.iq, [4] damian.giaouris@ncl.ac.uk
*Corresponding Author

***Abstract*—This study presents a design method for a voltage regulation system for a Boost converter that can be used in a power distribution unit within a power generation system. The regulation system is based on a hybrid, sensorless control approach, the structure of the controller is built based on the combination of PI and LQR controllers. The role of the new structural controller in improving the transient and steady-state response as well as enhancing the stability of the Boost converter output signal is studied. The states of the converter are estimated by Luenberger observer system, which is designed using pole placement (PP) technique. Mathematical model of the Boost converter with the hybrid LQR-PI controller is formulated. The gain parameters of the LQR-PI controller are obtained effectively by using Grey Wolf Optimizer (GWO) algorithm. In optimization process the GWO with an effective fitness function is used to tune the state and input weighting matrices of LQR controller. To validate the proposed control system a comparison between the performance of the LQR-PI controller and LQR controller with integral action (I) is achieved. The Boost converter circuit with feedback LQR-I/PI controllers are simulated utilizing Simulink software and their responses are assessed based on rise time, settling time overshoot and steady state error performance parameters. To verify the robustness of the control system, the performance of the converter is evaluated in five working scenarios under hard uncertainties in source voltage, reference voltage and resistive load. The simulation results demonstrate the effectiveness of the presented LQR-I/PI controllers in rejecting the effect of disturbances in the system response. However, the LQR-PI controller showed more accurate and stable output voltage compared to the LQR-I controller.**

Keywords—Hybrid Controller; Sensorless Control; Pole Placement Observer; Disturbance Rejection; Robust Voltage Regulation; Grey Wolf Optimizer, Uncertainties Parameters.

I. INTRODUCTION

Power converters play a prominent role in wide technical environments such as industrial applications, power distributed units and renewable systems. These applications need power converters with high performance and accurate output. Among these power devices the DC-DC converters, which perform an important role in the conversion and adaptation tasks of the energy level in numerous energy and industrial applications [1]-[3]. The DC-DC converters are mainly classified into six types: Buck-Boost, Buck, Boost, Zeta, Sepic, and Cuk [3], which considered are more power-efficient devices due to their high voltage conversion efficiency that reaches to 98%. Among these power devices is Boost converters that have a great and important influence in the operation of the energy systems as they can increase the power level between the power source and load ports of the energy system [4]-[7]. Boost converters enhance the power generated from the solar power source through increasing the PV power level and connecting it to off-grid or on-grid. Control of these power devices directly effects on the reliability and stability of the overall power system. This research is concerned with modeling a DC-DC Boost converter and developing a suitable control approach to ensure stability and a certain level of voltage manipulation performance by considering power problems and their applications.

To achieve this, improving converters performance and reducing static error has become the main goal of converter development. For this reason, many control techniques have been proposed during the last decades to stabilize the dynamic behavior of the Boost converters, such as classic control [8], [9], sliding mode control [10], boundary control [11], optimal control [12], robust control [13], adaptive control [14], [15], passivity based control [16], H∞ control [17] and back stepping control [18]. It is worth noting that the results of the above studies are based on the full information feedback control scheme, which means that all the system states are assumed measurable. However, current sensors and their conditioning circuits increase the complexity of implementation process, in addition cause extra hardware costs, delay and noise in the scheme response. Furthermore, it may also compromise the reliability of the power system. Therefore, it is recommended to implement current sensorless control strategies, not only to provide a reliable solution to control problems, but also to provide more effective solutions for Boost regulation problems.

These solutions make economic sense because they are based on the principle of reducing the number of system sensors and using a state observer that is used to estimate the unknown signals of the boost converter system. Moreover, the sensorless control method based on optimal

observer (Kalman Filter) can perform a disturbance rejection task along with the state estimation process for the realistic power converter systems [19], [20].

During the last decade, many researchers have conducted several interesting studies on sensorless control techniques with state estimator for DC-DC converter systems. In [21], the authors introduced the use of Boost converter circuit in various energy systems supplied by battery, wound rotor asynchronous motor, wind generator and solar panel module. This study focuses on design a sensorless controller for Boost converter system to avoid the need for the current sensor for the purpose of cost reduction and enhancing the reliability. They proposed PI Passivity-Based Control (PI-PBC) system to regulate the voltage signal in the output of the Boost converter. The value of the inductor current in the system is estimated by using Generalized Parameter Estimation-Based Observer (GPEBO). The estimation process is implemented based on Finite-Time Convergence (FTC) method that was adopted to enhance the system convergence. Mathematical aspects of the design procedure for both PI-PBC controller and GPEBO current estimator are presented. The proposed power system is simulated and the tracking performance of the GPEBO based PI-PBC sensorless controller is presented and analyzed based on variable source voltage scenario. Different observer gains are used in the assessment scenario of the GPEBO estimator. The robustness of the introduced system is evaluated in hard working scenario, in which the voltage regulation of the sensorless controller is tested under changing resistive load. The converter system is implemented experimentally in the real-time and its practical results are presented and analyzed to verify the proposed GPEBO based PI-PBC sensorless control system.

A sensorless disturbance rejection design in [22] is proposed for PWM DC-DC Buck and Buck/Boost converter. The converters are modeled and examined as a Markovian switching system. The authors introduced a predictive controller with a dynamic observer system to perform state estimation and stabilize the dynamic behavior of the converters. In this study, the estimator is adopted to support the two-mode tracking control method "voltage/current control" used to implement the converter regulation process by satisfying the terminal constraints for the presented tracking scheme. Two working scenarios are considered in this study in evaluation process of the proposed system regarding disturbance rejection and time-delay compensation.

A comparison between sensorless predictive control with observer and robust classical model predictive control strategies are presented and discussed. In the first scenario, the closed-loop Buck converter system based on the two strategies is targeted for fixed voltage/current values, 15V/1.25A. While in the second scenario, the Buck/Boost converter mode is designed to meet the target of the next sequence [15-23-10]V/[1.25-2.5-0.8]A. The comparison results showed the sensorless predictive controller with estimator compared to the classical MPC controller is more efficient in terms of the reference tracking, disturbance rejection and time–delay compensation.

In 2022, a sensorless control system using passivity-based controller with PI action is proposed to stabilize Cuk and Boost converters with exponential convergence [23]. A reduced-order GPEBO observer is introduced to reconstruct the non-measurable states and estimate the unknown value of the load conductance for the DC-DC converters. In this study, the observer was relied upon in performing finite-time convergence process, imposing the alertness preservation to be able to make an estimate for the time-varying load conductance and satisfying the excitation condition required in the power converters. The power converters with feedback observer based sensorless controller is simulated and implemented in the real-time domain. The simulated and experimental results are presented and then concluded to assess the effectiveness of the introduced control scheme and the estimation approach.

A voltage adjustment across unknown resistive loads for converters' topologies, Buck, Boost, Buck-Boost and non-inverting Buck-Boost is presented in [24]. The model of the converters have been formulated with a generalized port-Controlled Hamiltonian (PCH) representation. The authors based on the PCH formulation designed a passivity-based controller with PI action system to stabilize the output signal of the DC-DC converters. The value of the unknown resistive load is determined by utilizing integral estimator based adaptive estimator that is employed to decrease the number of sensors in the converters' models. A comparison between PI-PBC and the conventional PI controller is achieved for the converter's topologies under fixed desired voltage and load resistance changes condition. The simulated and experimental results demonstrated that the PI-PBC controller can lead to a better and more stable transient and steady state voltage regulation performance compared to the traditional PI controller.

An optimal closed-loop control system is introduced in [25] to stabilize the dynamic voltage behavior of Boost converters. The control system combines a linear state feedback controller technique with integral action. The state feedback controller is used to adjust the output voltage of the Boost regulator while the integral controller is adopted to decrease the error signal of the system response at steady state domain. The authors are also developed the proposed system by adding a state observer to the state feedback controller that comes with the advantages in estimating the unmeasurable load voltage and inductor current signals. Simulation findings of the voltage-controlled Boost converter were presented and evaluated in order to investigate the efficiency of the introduced sensorless state feedback control system.

In 2023, a study uses an Inverse Optimal Control (IOC) technique to adjust and stabilize output voltage signal of Boost regulator feeding an unknown DC resistive load [26]. The presented control method involves developing the control effort through the controller to ensure asymptotic stability in the converter output response, with the added benefit of including an integral parameter (I) without compromising stability. The authors introduced two estimators' techniques to reduce the number of measurement sensors needed to implement the I-IOC controller. The first state observer is based on the

Immersion and Invariance (I&I) approach that utilized to determine the load current, while the second estimator calculates the input voltage value using Disturbance Observer (DO) method. With the presence of estimators, the voltage regulation behavior of the presented sensorless controller is evaluated in simulation domain and then compared to that of Sliding-Mode Control (SMC). To validate the voltage regulation performance of the presented sensorless control system, it is implemented experimentally in a Plexim RT-Box. The practical findings are introduced and then analyzed to assess the dynamic behavior of the presented sensorless controller with integral action. This work is developed by [27], [28] to enhance the stability of the output voltage for Boost converter system by combining a nonlinear controller with state estimator based on I&I technique.

In most of the above studies the gain parameters of the proposed controllers were tuned using a trial and error method, which requires more effort and spends more time. Moreover, there is no guarantee that the parameter values obtained are the best among the range of available values of these parameters, and thus the system may not operate in the optimal condition [29], [30]. To avoid this drawback, evolutionary optimization techniques should be applied in order to find the optimal values of the Boost controller gains, thus improving the converter performance and increasing the regulation efficiency.

During the last decades, many computer-aided optimization algorithms have been introduced through numerous studies with the aim of improving the performance of controllers used in Boost converters, genetic algorithm (GA) [31] particle swarm optimization (PSO) [8], [31], bacteria foraging optimization algorithm (BFOA) [32], strength Pareto evolutionary algorithm (SPEA) [33], Cuckoo Optimization Algorithm (COA) [34], Firefly Algorithm (FA) [35] and Grey Wolf Optimizer (GWO) [36], [37].

In this research, a hybrid sensorless optimal controller is utilized to adjust output signal of the Boost converter system. The proposed controller for the Boost voltage control system is structured of a full state feedback LQR controller followed by PI controller. The adoption of this controller is due to its ability to achieve a compromise between the system response and the control effort. Following the optimal controller (LQR) by the PI control stage enhances the stability, improves the transient response and reduces the steady state error of the system response.

In the proposed system, it is assumed that the capacitor voltage and inductor current of the converter are non-measurable, hence, Luenberger observer technique is adopted to estimate those not available states signals. Luenberger observer has been first developed by Luenberger for linear control systems [38]. The voltage adjustment behavior of the presented LQR-PI controller with full state observer is optimized by utilizing the GWO tuning method.

The GWO tuning method is recommended to use in this study as it is flexible, scalable, easy to use and its ability to provide better results than traditional methods in terms of accuracy and speed when solving control problems involving multiple variables. In addition, the algorithm requires no derivation information of the search space, and it also has only a few parameters. Furthermore, this optimization algorithm exceeds the internal and local solutions and deals with single-objective problems [39]. However, this algorithm lacks the speed factor in performing its position update, which causes slow down the process of solving the control problem for complex dynamical systems (multiple-input, multi-output systems).

The proposed Boost converter system is simulated in the Matlab/Simulink toolbox to investigate the effectiveness of the proposed sensorless optimal control approach. The remainder of this research is structured as follows: section II presents mathematical modeling of the Boost dynamics in the state space representation form. Section III details the structure of the proposed LQR-PI controller and background of the control techniques. Section IV presents background and tuning procedure of the GWO algorithm used for controller optimization process. Design of the proposed Boost control system, including the mathematical formulation of the observer and the LQR controller with PI action is introduced in section V. Simulation results of the presented Boost converter system are shown and evaluated in section VI. Finally, the main concluding remarks and future works are introduced in section VII.

II. BOOST MODELING AND DESIGN

A. Boost Configuration and Modeling

The Boost converter is a step-up power regulator system that gets its name from its ability to convert a low-level DC input voltage into a higher-level DC output voltage. The electric circuit of a Boost converter is as shown in Fig. 1. The converter composes mainly of MOSFET power transistor (S), freewheel diode (D), inductor and capacitor, which represent two energy storages elements in the converter circuit, and finally resistive load.

The presence of capacitor and inductor elements makes the Boost converter nonlinear system as their current-voltage relationships are nonlinear and differential [40], [41]. In this study, the switching elements S and D operate in Continuous Conductance Mode (CCM). In this operation mode, the inductor current passes through the converter circuit continuously with low oscillation value [42], [43]. The behavior and operation of the voltage regulator depend on the switching states of the power transistor and the diode, which give two electric structures for the DC-DC Boost converter system. Transistor switching modes:

A. Switch-ON Mode

The equivalent electric circuit of Boost regulator during this switching case is shown in Fig. 2(a) [44], [45]. Using Kirchhoff's current and voltage laws, the inductor's current and capacitor's voltage of the Boost converter in the switch-ON state (S-ON) are stated in (1) and (2) respectively.

$$\frac{di_L}{dt} = \frac{1}{L} V_{in} \tag{1}$$

$$\frac{dV_c}{dt} = \frac{V_c}{RC} \tag{2}$$

The dynamic states of the regulator is the inductor's current and the capacitor's voltage $(x_1(t) = i_l(t), x_2(t) = v_c(t))$, the representation of the converter scheme in the state space form is expressed as follows:

$$\dot{x}_c(t) = A_c x(t) + B_c u(t) \quad (3)$$

$$y(t) = C_c x(t) \quad (4)$$

Where $x(t) = [x_1(t) \quad x_2(t)]^T$ is the state vector of the system, $u(t) = V_{in}$ is the input signal, A_c is the state matrix, B_c is the input matrix and C is the output matrix:

$A_c = \begin{bmatrix} 0 & 0 \\ 0 & \frac{1}{RC} \end{bmatrix}$, $B_c = \begin{bmatrix} \frac{1}{L} \\ 0 \end{bmatrix}$ and $C_c = [\,0 \quad 1]$.

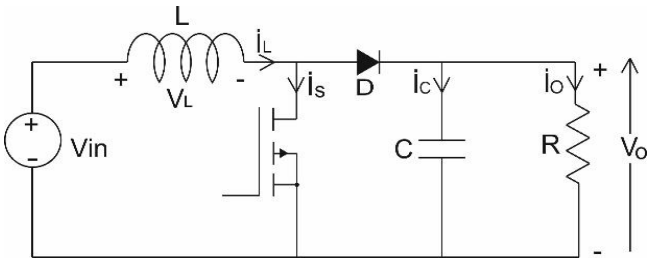

Fig. 1. Electric circuit of the boost converter

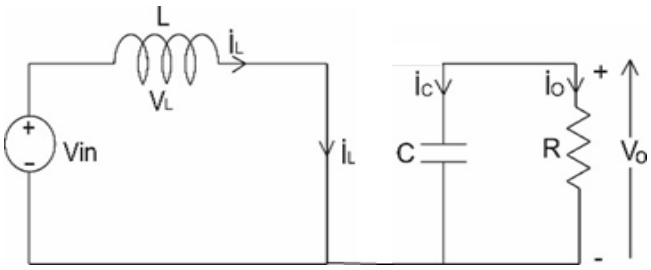

(a) ON switching state

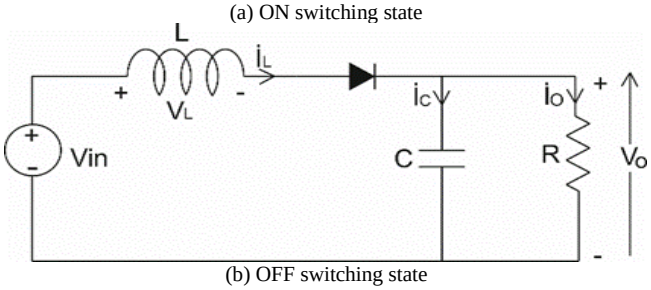

(b) OFF switching state

Fig. 2. Boost converter circuit based on transistor switching modes

B. Switch-OFF Mode

Fig. 2(b) shows the equivalent circuit of converter system during this switching period [44], [45]. A gain using Kirchhoff's current and voltage laws, the inductor's current and capacitor's voltage of the converter are given in (5) and (6) respectively.

$$\frac{di_L}{dt} = \frac{1}{L}V_{in} - \frac{1}{L}V_C \quad (5)$$

$$\frac{dV_c}{dt} = \frac{1}{C}i_L - \frac{1}{RC}V_c \quad (6)$$

Using (5) and (6), the state space representation of the converter during the switch-OFF state (S-OFF) is as follows:

$$\dot{x}_o(t) = A_o x(t) + B_o u(t) \quad (7)$$

$$y(t) = C_o x(t) \quad (8)$$

where the state matrix $A_o = \begin{bmatrix} 0 & -\frac{1}{L} \\ \frac{1}{C} & -\frac{1}{RC} \end{bmatrix}$, the input matrix $B_o = \begin{bmatrix} \frac{1}{L} \\ 0 \end{bmatrix}$, and the output matrix $C_o = C_c$.

Designing a LQR optimal control system for Boost regulator requires formulating a general state space representation for the converter model [46]. In this context, a general state, input and output matrices are formulated as follows using (3), (4), (7) and (8) through state space averaging technique.

$$A = A_c d + A_o(1-d) \quad (9)$$

$$B = B_c d + B_o(1-d) \quad (10)$$

$$C = C_c = C_o = [0 \quad 1] \quad (11)$$

where $A = \begin{bmatrix} 0 & -\frac{1-d}{L} \\ \frac{1-d}{C} & -\frac{1}{RC} \end{bmatrix}$, $B = \begin{bmatrix} \frac{1}{L} \\ 0 \end{bmatrix}$ and d is positive number less than one duty cycle, which governs the output signal of the Boost converter through the following expression:

$$V_o = \frac{Vin}{1-d} \quad (12)$$

Using (9)-(11), the general state equation and output equation of the Boost scheme are expressed as follows:

$$\dot{x}(t) = Ax(t) + Bu(t) \quad (13)$$

$$y(t) = Cx(t) \quad (14)$$

The values of the Boost parameters that have been used in this study are listed in Table I, where the converter is designed using [47] to equip a resistive load with DC power of approximately 30W. Considering all the parameters (Table I), the state and output matrices (13) and (14) are expressed as follows:

$$\begin{bmatrix} x_1(t) \\ x_2(t) \end{bmatrix} = \begin{bmatrix} 0 & -33.3 \\ 5400 & -600 \end{bmatrix} \begin{bmatrix} x_1(t) \\ x_2(t) \end{bmatrix} + \begin{bmatrix} 66.66 \\ 0 \end{bmatrix} u(t) \quad (15)$$

$$y(t) = [0 \quad 1] \begin{bmatrix} x_1(t) \\ x_2(t) \end{bmatrix} \quad (16)$$

TABLE I. PARAMETER VALUES OF THE BOOST CONVERTER

Parameter name	Symbol	Value	Unit
Input voltage	V_{in}	20	V
Output voltage	V_o	40	V
Load resistance	R_L	18	Ω
Switching frequency	F_s	10	kHz
Voltage ripple	Δ_v	3%	V
Current ripple	Δi	3%	A
Inductor	L	15	mH
Capacitor	C	92.59	μF

III. CONTROL STRUCTURE

In this study, a combination of LQR with PI controller is adopted in the control strategy of the proposed voltage regulation system for the Boost converter. The feedback

LQR controller is employed to control the performance of the Boost states. Whereas the proportional term (P) and integral term (I), are incorporated in the feedback loop of the Boost control system to enhance the stability achieved by the LQR controller and reject perturbations so that the overshoot and steady state error in the converter output is minimized as much as possible.

It is worth mentioning that in the practical systems not all the systems' states are always measurable or available. In this work, it is assumed that there is no measurement sensors are used in the Boost system, this assumption not only reduces the cost of the system but also overcomes the problem of measurement noise, which added to the system by these sensors devices. Therefore, a full-order observer system in this work is employed to estimate the states of the converter circuit. State feedback control approach based on the LQR and PP techniques are adopted to achieve the control and state estimation process in the presented voltage regulation system respectively.

A. LQR Technique

Generally, applying the LQR controller to regulate and stabilize the output voltage of Boost converter involves supplying the optimal state-feedback control effort [48]:

$$u(t) = r - Kx(t) \tag{17}$$

To the state and output equations that described previously in (13) and (14), where r is desired input and K is the gain matrix of the LQR controller. Fig. 3 illustrates block diagram of the converter control system based on LQR controller technique. To assign optimal control effort by which the performance the system is optimized, the following cost function [48], [49]:

$$J = \int_0^\infty [x^T(t)Qx(t) + u^T(t)Ru(t)]dt \tag{18}$$

Should be minimized. Where Q and R are two positive definit matrices that called state and input weighting matrices of the LQR controller respectively. These weighting matrices govern the gain matrix (K) of the LQR controller that can be obtained by the following expression:

$$K = R^{-1}B^TP \tag{19}$$

where P is the positive definite solution of the following Continuous Algebraic Riccati Equation (CARE) [19]-[22]**:**

$$A^TP + PA - PBR^{-1}B^TP + Q = 0 \tag{20}$$

B. PP Controller

Pole placement is a control technique by which it can calculate an optimal gain matrix that used to set the closed-loop poles of the controlled system at specific locations, thus ensuring system stability. For this to happen the plant of the system under consideration must be completely state controllable [50].

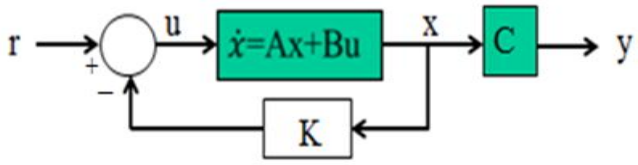

Fig. 3. Block diagram of LQR closed-loop control system

For n^{th}-order system with state space representation described by (13) and (14) to be completely controllable, the condition $\boldsymbol{rank}([\boldsymbol{B} \vdots \boldsymbol{AB} \vdots \boldsymbol{A^2B} \vdots \cdots \boldsymbol{A^{n-1}B}]) = \boldsymbol{n}$ should be satisfied. For a dynamic system that satisfies the controllability test, the control effort that places its closed loop poles to desired positions in a tracker problem can be calculated using the same mathematical formula for the LQR controller that was stated in the (17).

The term (K) in (17) based on pole placement technique is the state-feedback gain matrix ($1 \times n$), which is a row vector of constant gains that forces the closed-loop poles of the system to be located at the desired locations.

In this case study, the PP technique is adopted to design the estimator of the Boost converter system. Design process of PP based estimator system using characteristics equation of the system will be considered in section V in detail.

C. PI Controller

PI/PID controllers are mostly used in industrial applications, chemical processes, electrical and power systems because they are characterized by a simple design, ease of implementation, in addition to the ability to achieve good performance [51], [52]. The proportional parameter of the PI controller deals with the present error of the system output and governs response speed of the system. Whereas the integral parameter addresses the accumulated past error of the system response and gives a correction offset action required to overcome the steady state error in the system response. The time-domain expression of the PI command signal is given:

$$u(t) = K_pe(t) + K_i\int_0^t e(\tau)dt \tag{21}$$

Proper setting for the proportional and integral parameters and LQR weighting matrices (Q and R) which can enable the converter to provide an accurate and stable output voltage across the resistive load terminals.

IV. GWO ALGORITHM

GWO algorithm is a mathematical model of an optimization method that was inspired from the hunting behavior and leadership of grey wolves in the wild. Mirjalili first presented the GWO tuning algorithm in 2014 [53]. This optimization method has been successfully applied to perform an optimum tuning task for controller parameters in many control problems [54], [55]. The wolf pack when hunting prey are divided into four hierarchical groups based on their strength and fitness called alpha (α), beta (β), delta (δ) and omega (ω). Alpha is the fittest wolf in the pack, while beta includes the wolf group with fitness close to alpha wolf. Beta category consists of subordinate wolves,

and finally the rest of the pack are follower wolves which called omega.

In hunting process, alpha is the leader wolf who plays a prominent role for making important decisions regarding hunting the prey, sleeping place and attack time etc. The second level in the pack hierarchical, beta, helps the leader wolf in decision-making and other pack responsibilities. Delta group assists beta wolves in achieving their activities, whereas the wolves in the omega category follow all the orders given by the dominant wolves. The same procedure is considered in the GWO optimization method, which is adopted to fine-tune the Q and R elements of combined LQR-PI controller $(q_{11}, q_{22}, q_{33}, r)$ based on a certain objective function, which should be formulated under the required response parameters. In this work, the cost function (J) is formulated below in (22) based on the response parameters of the system in the transient and steady state domain, which are rise time (t_r), settling time (t_s), maximum overshoot (M_o) and steady state error (e_{ss}).

$$J = a_1 t_r + a_2 t_s + a_3 M_o + a_4 e_{ss} \tag{22}$$

where a_1, a_2, a_3 and a_4 are the weight values of the output response parameters for the converter system numbers with values which, are chosen in this study 0.2, 0.2, 0.2 and 0.4 respectively. The tuning procedure of the presented GWO algorithm for the coefficients of the hybrid state feedback controller is summed as:

- Define the state space model of the Boost regulator.
- Define the coefficients of the controller $(q_{11}, q_{22}, q_{33}, r)$.
- Define the objective function of the control problem (J).
- Define the position parameters of the GWO algorithm (α, β, δ).
- Initialize the algorithm population (n), iteration number i.
- Initialize α, β and δ values.
- Run the iteration sequence of the algorithm.
- Update the position values of the wolves.
- Calculate the value of the objective function for the current position.
- Site update for the rest of the wolf pack.
- Calculate the new position of the α wolf.
- Update the position of the α wolf.
- The optimum solution is the last updated position of α wolf.

The mathematical expressions of the GWO algorithm in obtaining an optimal solution for the converter problem are given below [56], [57]. For k^{th} iteration:

$$\vec{X}(k+1) = \vec{X}_p(k) - \vec{A}\vec{D} \tag{23}$$

$$\vec{D} = \vec{C}\vec{X}_p(k) - \vec{X}(k) \tag{24}$$

where $\vec{X}(k+1)$ denotes the position vector of the current solution (wolf position vector), $\vec{X}_p(k)$ indicates the position of the optimum solution (vector position of the prey), k represents the current iteration, $\vec{A}, \vec{C}$ and $\vec{D}$ represent vectors of problem coefficients, and these vectors are calculated using the following formula:

$$\vec{A} = 2\vec{a}r_1 - \vec{a} \tag{25}$$

$$\vec{C} = 2r_2 \tag{26}$$

where a is a vector whose elements values decrease linearly from 2 to 0 as the algorithm iterations proceed and r_1 and r_2 are randomly chosen number between 0 and 1. The a vector is decreased based on the (27).

$$\vec{a} = 2 - k\frac{2}{t} \tag{27}$$

The expression of the new solution (new position vector) is below given:

$$\vec{X}_i(k+1) = \frac{X_{i1}(k) + X_{i2}(k) + X_{i3}(k)}{3} \tag{28}$$

$$\left.\begin{aligned} \vec{X}_{i1}(k) &= \vec{X}_\alpha(k) - \vec{A}_1 D_\alpha \\ \vec{X}_{i2}(k) &= \vec{X}_\beta(k) - \vec{A}_2 D_\beta \\ \vec{X}_{i3}(k) &= \vec{X}_\delta(k) - \vec{A}_{31} D_\delta \end{aligned}\right\} \tag{29}$$

$$\left.\begin{aligned} \vec{D}_\alpha &= \vec{C}\vec{X}_\alpha(k) - \vec{X}_{i1} \\ \vec{D}_\beta &= \vec{C}\vec{X}_\beta(k) - \vec{X}_{i2} \\ \vec{D}_\delta &= \vec{C}\vec{X}_\delta(k) - \vec{X}_{i3} \end{aligned}\right\} \tag{30}$$

where $\vec{X}_i(k+1)$ is the best solution relative to optimum solution (it is the wolf that has the optimum location relative to the prey) and i is the current number of algorithm iteration.

To achieve a good solution for control problem, th parameters of the GWO algorithm should be selected properly, selection of the number of wolfs could change the convergence speed and has an impact on the capability of the GWO to provide best solution for the control problem. Using only a few number of wolfs could lead to the worst solutions thereby, obtaining worse system results because relying a few wolves cannot adequately represent the chain of command and explore the search space. While using too many wolves can decrease the impact of encircling prey and attacking mechanisms. For that adopting a reasonable number of wolves (50 wolf) not only can sufficiently explore the search space but also fairly benefit from surrounding the prey and attacking mechanisms, hence achieving optimum solution for the control problem [58].

V. BOOST CONTROL SYSTEM DESIGN

In this study, LQR with PI control approach is recommended to manage the performance of voltage regulation process for the Boost converter system. The hybrid controller receives the error signal between the desired signal and the Boost output signal and sends an

adjustable duty cycle PWM control signal to the MOSFET power switch of the voltage regulator. The PWM command signal controls the dynamic behavior of the converter and force its output to follow the desired signal trajectory.

A. Observer Design

Adopting full state feedback controller technique to regulate and stabilize the output signal of Boost converters requires all states of the system be available. However, practically some of those states may be not available. Therefore, to enable design the controller all the non-measurable states of the converter system must be estimated properly. In this study, it is assumed the capacitor voltage and the inductor current signals of the converter are not available as the proposed system is not equipped with signal sensors devices, which add to the system unwanted noise signal that categorized as measurement noise, hence the system is free from this external disturbance type. It is worth considering that, there is another external disturbance source which, is classified as process noise that comes from the inaccuracy of the system model, the effect of this noise type is assumed in this study case is small and therefore it is omitted. For the purpose of Boost control system design, Luenberger observer technique, which was found by Luenberger in 1971 [59], is employed for estimation of the unknown system states.

For the Boost converter with continuous Linear Time Invariant (LTI) model stated in (13) (14), a linear observer system is given below [60]:

$$\dot{\hat{x}}\,(t) = A\hat{x}(t) + Bu(t) + K_e\big(y(t) - \hat{y}(t\,)\big) \tag{31}$$

$$\hat{y}(t) = C\hat{x}(t) \tag{32}$$

where $\hat{x}(t)$ is the estimated state vector of the plant state vector $x(t)$, $\hat{y}(t\,)$ is the estimated output of the system, and $K_e = [k_{e1} \quad k_{e2}]^T$ is gain matrix of the observer. The block diagram of the state observer is illustrated in Fig. 4. The estimation error is defined as:

$$e(t) = x(t) - \hat{x}(t\,) \tag{33}$$

Differentiation (33) yields:

$$\dot{e}(t) = \dot{x}(t) - \dot{\hat{x}}\,(t) \tag{34}$$

Substituting (13) and (31) into (34) gives:

$$\dot{e}(t) = A\big(x(t) - \hat{x}(t\,)\big) - K_e\big(y(t) - \hat{y}(t\,)\big) \tag{35}$$

With (14) and (29), the above equation becomes:

$$\dot{e}(t) = A\big(x(t) - \hat{x}(t\,)\big) - K_eC\big(x(t) - \hat{x}(t\,)\big) \tag{36}$$

Based on (31), the differential expression for the system error becomes:

$$\dot{e}(t) = (A - K_eC)e(t) \tag{37}$$

Solution of (34) is given in (38):

$$e(t) = e^{(A - K_eC)}e(0) \tag{38}$$

When the time (t) approaches to zero the error of estimation approaches to zero. The stability of the state estimator is governed by the eigenvalues of the observer state matrix $(A - K_eC)$, which can be achieved arbitrary by appropriate choice of the observer gain matrix (K_e) when the pair matrix $[A, C]$ satisfies the observabilty test.

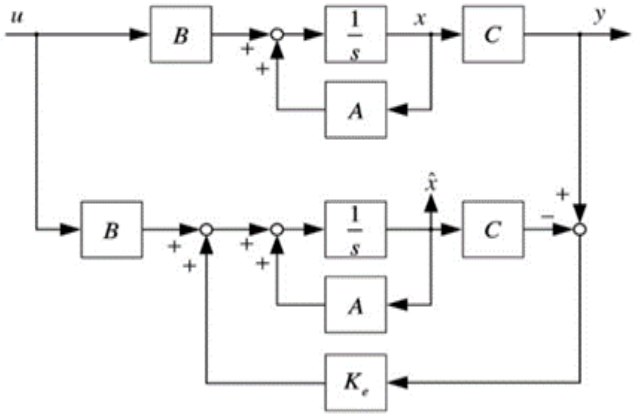

Fig. 4. Schematic diagram of state observer

For designing a state observer it is required to know the dynamics of the plant, defined by the poles of the converter, which can be obtained with the following characteristic polynomial:

$$|sI - \mathrm{A}| = s^2 + \alpha_1 s + \alpha_0 \tag{39}$$

It is worth noting that, in software it can easily find the eigenvalues of the Boost plant by the Matlab command "*eig*", the obtained poles of the converter are: $[-300 \pm 299.7i]$. Regarding the observer, it can be designed using the direct comparison method where the value of the gain matrix is determined using the following characteristics equation:

$$|sI - A + K_eC| = (s - \mu_1)(s - \mu_2) \tag{40}$$

where μ_1 and μ_2 are the desired closed-loop poles of the observer scheme, which should be located far away from the imaginary axis. The gain of the estimator is designed in such a way that the estimator responds fasters than the Boost converter response [61], [62]. For that the poles of the observer should 5 times bigger than the dominant pole of the converter. In this research, the gain matrix of the observer is determined using the Matlab command "*place*" based on the best pole values that were obtained using the GWO algorithm. In addition, the gain matrix can also be calculated using the Matlab command "*acker*" based on the same procedure [62], [63].

B. Boost Controller Design

In this work, state feedback control based on the LQR controller is adopted to control the dynamics of the introduced Boost converter scheme. A PI controller is combined with the LQR controller in the presented control approach to enhance the stability of the converter performance and improve its transient and steady state response. Including the integrator to the control system of the Boost regulator can reduce the error of the system response in the steady-state response domain, however, it also will add an extra state to the converter plant [45], [64]. Fig. 5 shows the block diagram of complete Boost hybrid sensorless control system with estimator. The presented system is augmented by including the error signal as an

additional state into the Boost scheme states. The state vector of the proposed system is given below:

$$x(t) = [i_L \;\; v_R \;\; z]^T \tag{41}$$

where z is error signal that is defined as below:

$$z = \int_0^t (v_{ref} - v_R)dt \tag{42}$$

The state feedback control law is given as:

$$u(t) = -Kx(t) + K_p\dot{z}(t) + K_i z(t) \tag{43}$$

where K is the LQR gain matrix of the Boost converter represented by: $K = [k_1 \;\; k_2]$ and K_p and K_i are the proportional and integral gain parameters of the PI controller respectively.

$$\dot{z}(t) = r - y(t) = r - Cx(t) \tag{44}$$

Substitute (44) in (43) yields:

$$u(t) = -Kx(t) + K_i z(t) + K_p(r - Cx(t)) \tag{45}$$

$$u(t) = -(K + CK_p)x(t) + K_i z(t) + K_p r \tag{46}$$

Using (43), the Boost state equation (13) can be reformulated as follows:

$$\dot{x}(t) = (A - BK - BCK_p)x(t) + BK_i z(t) + BK_p r \tag{47}$$

Based on (44) and (47), the state space formulation of the Boost scheme with the LQR-PI controller is given below:

$$\begin{bmatrix}\dot{x}(t)\\ \dot{z}(t)\end{bmatrix} = \begin{bmatrix}A - BK - BCK_p & BK_i\\ -C & 0\end{bmatrix} x_c(t) + \begin{bmatrix}BK_p\\ 1\end{bmatrix} r \tag{48}$$

$$y(t) = [C \;\; 0]\, x_c(t) \tag{49}$$

where $x_c(t) = [x(t) \;\; z(t)]^T$, the control effort of the closed-loop control scheme stated in (46) can be rewritten as follows:

$$u(t) = -\begin{bmatrix}K + CK_p & -K_i\end{bmatrix} x_c(t) + K_p r \tag{50}$$

$$u(t) = -\bar{K} x_c(t) + BK_p r \tag{51}$$

where $\bar{K} = [K + CK_p \;\; -K_i]$ is the gain matrix of the state LQR with PI controller. The state space representation of the closed-loop Boost's dynamics (46) can be written as follows:

$$\dot{x}_c(t) = [\bar{A} - \bar{B}\bar{K}]x_c(t) + \begin{bmatrix}BK_p\\ 1\end{bmatrix} r \tag{52}$$

$$y(t) = \bar{C}\, x_c(t) \tag{53}$$

The matrices $\bar{A}$, $\bar{B}$ and $\bar{C}$ are given by: $\bar{A} = \begin{bmatrix}A & \Theta\\ -C & 0\end{bmatrix}$, $\bar{B} = \begin{bmatrix}B\\ 0\end{bmatrix}$ and $\bar{C} = [C \;\; 0]$, where Θ is an (2x1) vector of zeros. Based on output matrix $C = [c_1 \;\; c_2]^T$, the LQR-PI controller gain matrix can be expressed as: $\bar{K} = [k_1 + c_1K_p \;\; k_2 + c_2K_p \;\; -K_i]$. In this article, the presented control system is designed on the basis that the output controlled signal is the load voltage of the Boost regulator circuit, hence the output matrix of the system is $C = [0 \;\; 1]^T$, and thus the gain matrix of the LQR-PI controller becomes: $\bar{K} = [k_1 \;\; k_2 + K_p \;\; -K_i]$.

The gain matrix of the proposed hybrid controller can be determined utilizing the Matlab command "*lqr*" based on the state weighting matrix (Q) = blkdiag(q_{11}, q_{22}, q_{33}) and input weighting matrix (R) = (r_{11}). In this study, the elements of Q and R matrices are tuned effectively by the GWO algorithm.

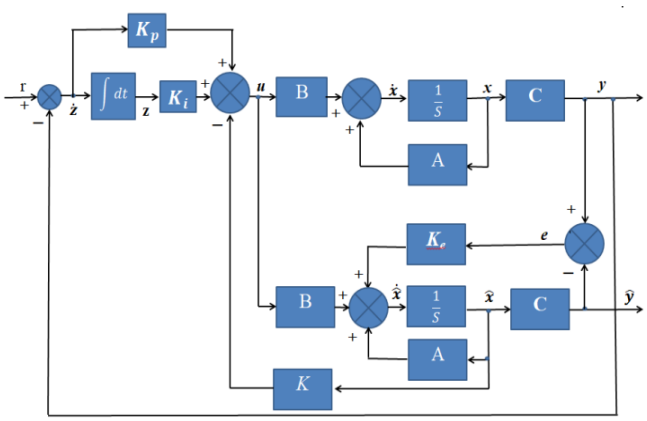

Fig. 5. Block diagram of hybrid control scheme using LQR-PI controller

VI. SYSTEM SIMULATION RESULTS AND DISCUSSIONS

The new approach of the sensorless control scheme is simulated utilizing the Matlab/Simulink software. The Simulink model of the state estimator-based Boost voltage regulator with LQR-PI controller is shown in Fig. 6. The proposed system is designed under certain desired performance specifications, rise time of 0.01s, settling time of 0.1s, maximum overshoot of 10% and static error of 0.1%.

In this study, GWO algorithm with parameters stated in Table II is firstly utilized to tune the LQR weighting matrices (Q, R) of the combined LQR-PI controller. Based on the optimized LQR-PI weighting matrices, the gain vector of the hybrid sensorless controller is obtained using the Matlab command "*lqr*" , $\bar{K} = \begin{bmatrix}k_1 & k_2 + K_p & -K_i\end{bmatrix} = [2.216 \; 0.027 - \; 2.2248]$. It is worth considering that the second component of $\bar{K}$ is sum of the two gain elements k_2 and K_p, in this context, the GWO algorithm in this study is applied again with problem dimension (d_m) of 2 (k_2, K_p) to extract the value of K_p from the generated gain component $(k_2 + K_p)$. The final LQR gain matrix is [2.2161 0.023933] while the PI gain parameters are $K_p = 0.0038892$ and $K_i = 2.2248$. Regarding the observer, the estimation process is implemented utilizing the PP technique. The gain matrix of the state observer is calculated using the Matlab command "*place*".

The calculation of the estimator gain matrix depends on the observer poles $(A - K_eC)$, which are chosen 5 times bigger than the dominant poles of the system. The eigenvalues of the observer is chosen (-1500$\pm$1500i), from this, the obtained observer gain matrix is $K_e = [800 \;\; 2400]^T$. To investigate the effectiveness of the proposed sensorless control system, the voltage regulation behavior of the LQR-PI controller is tested and compared with that of LQR-I controller under the following five working scenarios.

TABLE II. GWO ALGORITHM PARAMETERS FOR LQR-PI CONTROLLER

Parameter name	Symbol	Value
Population size	N	50
Iteration number	i	100
Problem dimension	d_m	4
Lower bound	lb	[0,0,0,0]
Upper bound	ub	[10,5,3,10]

A. Case 1: Certain Boost Parameters

In this first working case, the simulation of the Boost control scheme is implemented under normal working conditions where neither uncertainty nor any disturbance in the converter parameters was introduced. The voltage adjustment process of the Boost converter is evaluated for tracking the desired voltage of 30V under normal converter parameters, supply voltage of 20V, and load resistance of 26Ω. The tracking performance of the Boost regulator under action of the combined LQR-PI controller and LQR-I controller with state estimation system are shown in Fig. 7. The miniplot of the system output response demonstrates that both optimized controllers PSO-LQR-I and PSO-LQR_PI were able to provide a good reference tracking with a rise time of 0.1s and minimal steady state error less than the adopted values in the converter design process. However, compared to LQR-I controller, the LQR-PI controller reduced the settling time from 0.7s to 0.3s.

B. Case 2: Variable Reference Voltage

In this working case, the voltage regulation ability of the hybrid sensorless controller is tested at certain supply voltage of 20V, load resistance of 26Ω and hard disturbance in the reference voltage. Sharp change desired voltage and output waveforms of the Boost converter by means of LQR-I and LQR-PI controllers are shown in Fig. 8. Based on the simulated results, it can be said that both sensorless controllers succeeded in making the converter output follows the varying reference voltage signal efficiently.

It can also be noted from the miniplot of Fig. 8 that the LQR-PI controller shows a faster rise time compared to the LQR-I controller. The converter output based on the LQR-I and LQR-PI control strategies takes time approximately 0.06s and 0.03s respectively to reach its acceptable steady state value. However, there is an overshoot of approximately 5% at fall state of the output response. It can be concluded that both controllers still show an acceptable response and good tracking of the desired input trajectory in a turbulent environment, especially the LQR-PI controller.

C. Case 3: Variable Source Voltage

The performance of the presented control systems is assessed based different values of input voltage under a reference voltage of 30V. Fig. 9 displays the voltage value variation of the Boost power supply. Using the hybrid optimal controller approaches LQR-I and LQR-PI the output response of the Boost regulator system is presented in Fig. 10. The waveforms of the system response reveal the activity of the presented controllers to guide the Boost output signal through the trajectory of the reference input effectively. However, the LQR-PI controller showed more stable and better tracking performance, the output signal, not like using the LQR-I controller, oscillated symmetrically within the acceptable bound around the desired input.

D. Case 4: Variable Load Resistance

In this working scenario, the tracking behavior of the introduced sensoreless controllers has been investigated at the certain supply voltage of 20V and desired voltage 30V considering a sharp disturbance in the converter load resistance. Fig. 11 shows the output voltage waveform of the Boost regulator with the LQR_I/PI control strategies. It is clear from the output waveforms of the system that both controllers still show an acceptable response and closer tracking performance while retaining the advantage of the LQR-PI controller, which reduced the settling time from 0.25s to 0.1s compared to the LQR-I controller. However, the two controllers caused instantaneous overshoots at the time of change in load resistance, the effect of these overshoots can be neglected due to their short period.

E. Case 5: Variable Input, Reference and Load Resistance

The robustness properties of the two optimal control approaches were further evaluated under severe operating conditions, which include reference and supply voltage disturbance and load uncertainty. Fig. 12 presents the output response of the Boost regulator based on the LQR_I and LQR_PI controllers. It is clear from the output waveforms that the two controllers showed good response and effectively tracked the desired value of the system. The controllers showed fast response and oscillations with magnitude changed within the designer preference value. However, from the miniplots in Fig. 12 it can also be seen that the response obtained by the LQR_PI is better than that based on the LQR-I controller in both the transient and steady state response domain. The settling time for LQR-PI controller is 0.04s while for LQR-I controller is 0.07s, the overshoot percentage after 1s for LQR-PI and LQR-I controllers are 2% and 7% respectively. In steady state response domain, the value of fluctuation in the output response for LQR-PI and LQR-I controllers are ± 0.75V and ± 0.25V respectively with same error steady state value approximately of 5mV.

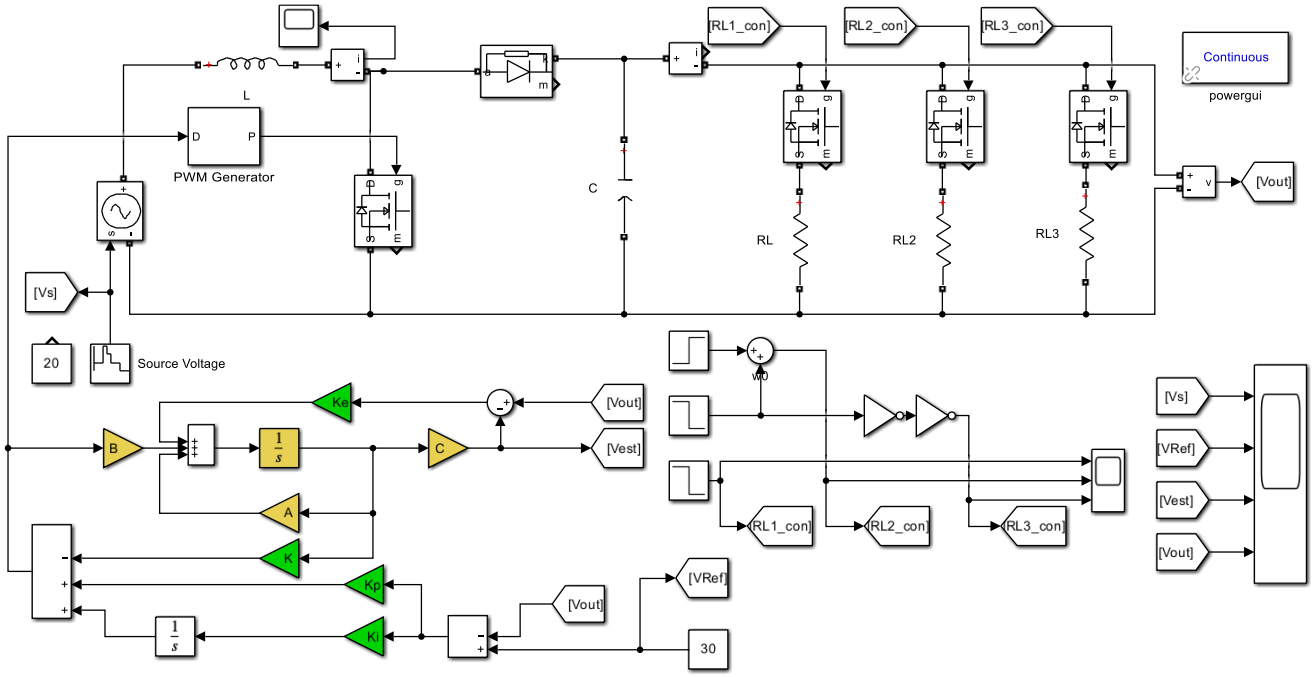

Fig. 6. Simulink model of the LQR-PI controller for Boost converter

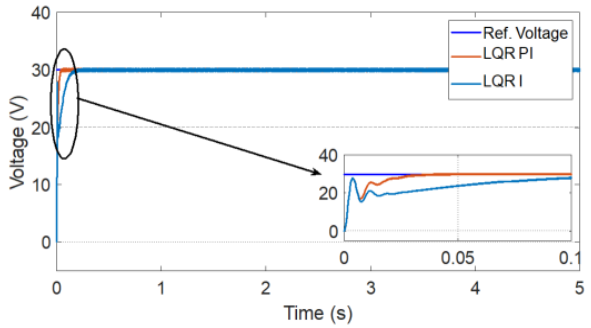

Fig. 7. Boost response under certain parameters

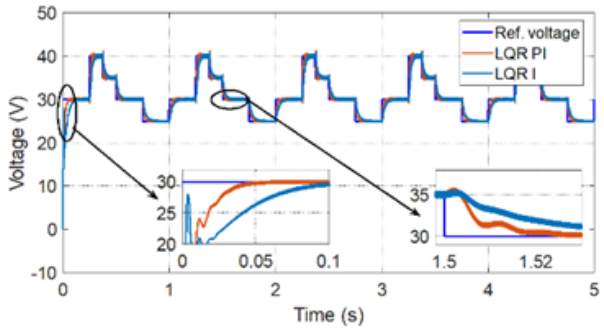

Fig. 8. Boost response under variable ref. voltage

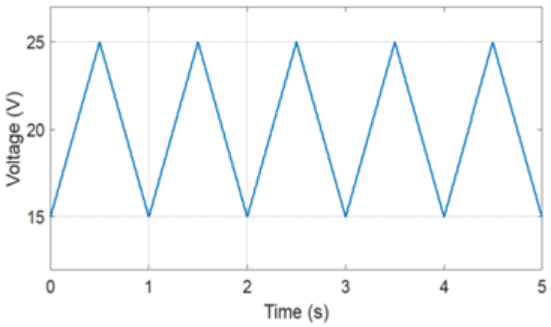

Fig. 9. Source voltage waveform

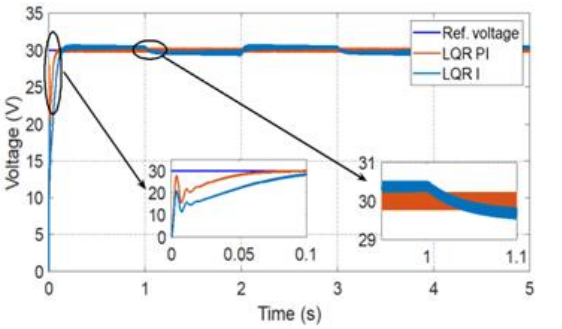

Fig. 10. Boost response under variable source voltage

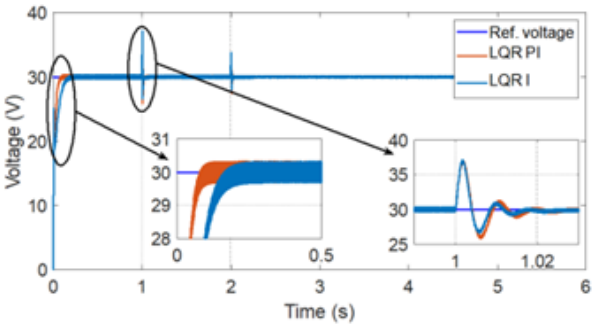

Fig. 11. Boost response based on uncertain load and source

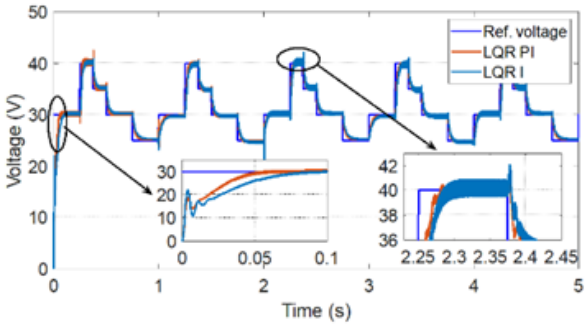

Fig. 12. Boost response based on variable and reference voltage

It is worth considering that the improvement achieved in the performance of the boost converter by the proposed voltage regulation system can enhance the role of the power electronic in renewable energy systems and electrical vehicles and many industrial applications.

VII. CONCLUSION

The main contribution of this study is to perform an effective regulation for the output voltage of non-measurable DC-DC Boost converter using hybrid optimal control systems based on the LQR controller technique. LQR with integral was used to improve the stabilization process and reduce the steady state error of control problems. A new hybrid optimal control approach, LQR with Proportional-Integral, was also presented in this work to enhance the stability and improve the transient and steady state response of the Boost regulator. The mathematical model of the LQR-PI control system was derived and presented, which was adopted in the design process of the controller gain elements.

Full-state estimation system based on the Luenberger observer technique was used to estimate the current and voltage states of the proposed non-measurable Boost converter system. Best values for the gain elements of the hybrid controllers were obtained by using GWO optimization method. The performance of the LQR_I and LQR-PI controllers were examined with supply and reference voltage disturbances and load resistance variation to investigate the effectiveness of the presented controllers.

Simulation results revealed that the unmeasurable system states, under the action of the Luenberger observer technique, achieved rapid and accurate convergence to their desired state values. Simulink findings also demonstrated that the two sensorless control methods (LQR-I/PI) successfully controlled the Boost converter regulation behavior and were able to stabilize the converter output voltage at the desired reference values under conditions of voltage and load uncertainty. As a comparison it can be pointed out that the LQR-PI sensorless controller achieved faster and more accurate tracking performance for the reference input trajectory and more effectively kept the stability of the output voltage through the steady-state response domain compared to the LQR_I controller.

In the predictive works, the reliability of the proposed system will be enhanced by considering external disturbances and process noise in the system modeling, and then a robust control system will be designed to deal with the system noise and uncertainty and provide a stable output response. In addition, the proposed Boost converter circuit with sensorless hybrid control system will be validated through the practical implementation of the system.

REFERENCES

[1] M. Harfman Todorovic, L. Palma, and P. N. Enjeti, "Design of a Wide Input Range DC–DC Converter With a Robust Power Control Scheme Suitable for Fuel Cell Power Conversion," *IEEE Transactions on Industrial Electronics*, vol. 55, no. 3, pp. 1247-1255, 2008.

[2] V. Viswanatha and R. Reddy, "Microcontroller based bidirectional buck boost converter for photo-voltaic power plant," *Journal of Electrical Systems and Information Technology*, vol. 5, no. 3, pp. 745–758, 2018.

[3] I. Mohammed and L. Khalaf, "Design and Simulation of an Analog Robust Control for a Realistic Buck Converter Model," *Journal of Robotics and Control (JRC*), vol. 5, no. 5, pp. 1336-1348, 2024.

[4] K. I. Hwu and Y.T. Yau, "Performance enhancement of boost converter based on PID controller plus linear-to-nonlinear translator," *IEEE Transactions on Power Electronics*, vol. 25, no. 5, pp. 1351–1361, 2009.

[5] Xu. Quinten, W. Jiang, F. Blaabjerg, Ch. Zhang, X. Zhang, and T. Fernando, "Backstepping control for large signal stability of high boost ratio interleaved converter interfaced DC microgrids with constant power loads," *IEEE Transactions on Power Electronics*, vol. 35, no. 5, pp. 5397–5407, 2019.

[6] W. He and R. Ortega, "Design and implementation of adaptive energy shaping control for DC–DC converters with constant power loads," *IEEE Transactions on Industrial Informatics*, vol. 16, no. 8, pp. 5053–5064, 2019.

[7] H. Wei, L. Shihua, Y. Jun, and W. Zuo, "Incremental passivity-based control for DC-DC boost converters under time-varying disturbances via a generalized proportional integral observer," *Journal of Power Electronics*, vol. 18, no.1, pp. 147–169, 2018.

[8] S. I. Saadi and I. K. Mohammed, "Power Control Approach for PV Panel System Based on PSO and INC Optimization Algorithms," *Journal Europeen des Systemes Automatises*, vol. 55, no. 6, pp. 825–843, 2022.

[9] I. K. Mohammed, "Design and Simulation of Voltage Control System for Simscape Boost Converter Model With Disturbances," *International Journal of Control, Automation and Systems*, vol. 22, no. 5, pp. 1707-1716, 2024.

[10] S. Oucheriah and L. Guo, "PWM-based adaptive sliding-mode control for boost DC–DC converters," *IEEE Transactions on Industrial electronics*, vol. 60, no. 8, pp. 3291–3294, 2012.

[11] T. -T. Song and H. S. -h. Chung, "Boundary Control of Boost Converters Using State-Energy Plane," *IEEE Transactions on Power Electronics*, vol. 23, no. 2, pp. 551-563, 2008.

[12] A. Brahimi, D. Kerdoun, and A. Boumassata, "Boost Converter Control using LQR and P&O Technique for Maximum Power Point Tracking," *19th International Multi-Conference on Systems, Signals & Devices (SSD)*, pp. 1998-2003, 2022.

[13] C. Tse, S. Wong, and S. Tan, "A unified approach for the derivation of robust control for boost PFC converters," *IEEE Transactions Power Electron*, vol. 24, no. 11, pp. 2531–2544, 2009.

[14] G. Song, X. Liu, G. Xiao, B. Chen, and P. Wang, "Decentralized Adaptive Control Strategy of DC-DC Boost Converter for Hybrid Energy Storage Systems Feeding CPLs," *IEEE Journal of Emerging and Selected Topics in Power Electronics*, vol. 12, no. 4, pp. 3663-3674, 2024.

[15] U. Saha, S. Shahria, and A. B. M. H. -U. Rashid, "Intelligent Control Strategies for DC-DC Boost Converter: Performance Analysis and Optimization," *2023 International Conference on Smart Systems for applications in Electrical Sciences (ICSSES)*, pp. 1-6, 2023.

[16] Y. I. Son and I. H. Kim, "Complementary PID Controller to Passivity-Based Nonlinear Control of Boost Converters With Inductor Resistance," *IEEE Transactions on Control Systems Technology*, vol. 20, no. 3, pp. 826-834, 2012.

[17] R. Naim, G. Weiss, and S. Ben-Yaakov, "H/sup /spl infin// control applied to boost power converters," *IEEE Transactions on Power Electronics*, vol. 12, no. 4, pp. 677-683, 1997.

[18] H. El Fadil and F. Giri, "Backstepping based control of PWM DC-DC boost power converters," *Proceedings of the 2007 IEEE International Symposium on Industrial Electronics*, pp. 395-400, 2007.

[19] Q. Tong, Ch. Chen, and Q. Zhang, "A sensorless predictive current controlled boost converter by using an EKF with load variation effect elimination function," *Sensors*, vol. 15, no. 5, pp. 9986-10003, 2015.

[20] A. G. Beccuti, S. Mariethoz, S. Cliquennois, S. Wang, and M. Morari, "Explicit Model Predictive Control of DC–DC Switched-Mode Power Supplies With Extended Kalman Filtering," *IEEE Transactions on Industrial Electronics*, vol. 56, no. 6, pp. 1864-1874, 2009.

[21] X. Zhang, M. Martinez-Lopez, W. He, Y. Shang, C. Jiang, and J. Moreno-Valenzuela, "Sensorless control for DC–DC boost converter

via generalized parameter estimation-based observer," *Applied Sciences*, vol. 11, no. 16, p. 7761, 2021.

[22] A Zahaf, S Bououden, M Chadli, I Boulkaibet, B Neji, and N Khezami, "Dynamic Sensorless Control Approach for Markovian Switching Systems Applied to PWM DC–DC Converters with Time-Delay and Partial Input Saturation," *Sensors*, vol. 23, no. 15, p. 6936, 2023.

[23] W. He, M. Namazi, T. Li, and R. Ortega, "A State Observer for Sensorless Control of Power Converters With Unknown Load Conductance," *IEEE Transactions on Power Electronics*, vol. 37, no. 8, pp. 9187-9199, 2022.

[24] W. González, O. Montoya, C. Restrepo, and J. Hernández, "Sensorless adaptive voltage control for classical DC-DC converters feeding unknown loads: a generalized PI passivity-based approach," *Sensors*, vol. 21, no. 19, p. 6367, 2021.

[25] T. Djamel, T. Amieur, B. Mohcene, and S. Kahla, "Sensorless Control of DC-DC Converter Using Integral State Feedback Controller and Luenberger Observer," *International Conference on Digital Technologies and Applications*, vol. 26, no. 1, pp. 1477-1488, 2021.

[26] O. Montoya, W. González, S. Riffo, C. Restrepo, and C.-Castaño, "A Sensorless Inverse Optimal Control Plus Integral Action to Regulate the Output Voltage in a Boost Converter Supplying an Unknown DC Load," *IEEE Access*, vol. 11, pp. 49833-49845, 2023.

[27] M. Malekzadeh, A. Khosravi, and M. Tavan, "A novel sensorless control scheme for DC-DC boost converter with global exponential stability," *European Physics Journal Plus*, vol. 134, no. 338, pp. 1-15, 2019.

[28] M. Malekzadeh, A. Khosravi, and M. Tavan, "A novel adaptive output feedback control for DC–DC boost converter using immersion and invariance observer," *Evolving System*, vol. 11, pp. 707–715, 2020.

[29] I. K. Mohammed, "Design of Optimized PID Controller Based on ABC Algorithm for Buck Converters with Uncertainties," *Journal of Engineering Science and Technology*, vol. 16, no. 5, pp. 404-4059, 2021.

[30] M. N. Ahmed, I. K. Mohammed, and A. T. Younis, "Design and Implementation of PSO/ABC Tunned PID Controller for Buck Converters," *Periodicals of Engineering and Natural Sciences (PEN)*, vol. 9, no. 4, pp. 643–656, 2021.

[31] J. Águila-León, C. D. Chiñas-Palacios, C. Vargas-Salgado, E. Hurtado-Perez, and E. X. M. García, "Optimal PID Parameters Tunning for a DC-DC Boost Converter: A Performance Comparative Using Grey Wolf Optimizer, Particle Swarm Optimization and Genetic Algorithms," *2020 IEEE Conference on Technologies for Sustainability (SusTech)*, pp. 1-6, 2020.

[32] N. Sudhakar, N. Rajasekar, S. Akhil, and K. J. Reddy, "Chaos control in solar fed DC-DC Boost converter by optimal parameters using nelder-mead algorithm powered enhanced BFOA," *IOP Conference Series: Materials Science and Engineering*, vol. 263, no. 5, pp. 1–22, 2017.

[33] A. Ahmadreza, R. Mohammadreza, T. Kambiz, G. Giovanni, and B. Issa, "Optimum design of integer and fractional-order PID controllers for Boost converter using SPEA look-up tables," *Journal of Power Electronics*, vol. 15, no. 1, pp. 160–176, 2015.

[34] A. Mamizadeh, N. Genc, and R. Rajabioun, "Optimal Tuning of PI Controller for Boost DC-DC Converters Based on Cuckoo Optimization Algorithm," *2018 7th International Conference on Renewable Energy Research and Applications (ICRERA)*, pp. 677-680, 2018.

[35] U. Saha, S. Shahria, and A. B. M. H. -U. Rashid, "Intelligent Control Strategies for DC-DC Boost Converter: Performance Analysis and Optimization," *2023 International Conference on Smart Systems for applications in Electrical Sciences (ICSSES)*, pp. 1-6, 2023.

[36] J. Águila-León, C. D. Chiñas-Palacios, C. Vargas-Salgado, E. Hurtado-Perez, and E. X. M. García, "Optimal PID Parameters Tunning for a DC-DC Boost Converter: A Performance Comparative Using Grey Wolf Optimizer, Particle Swarm Optimization and Genetic Algorithms," *2020 IEEE Conference on Technologies for Sustainability (SusTech)*, pp. 1-6, 2020.

[37] H. Shayeghi, R. Mohajery, N. Bizon, P. Thounthong, and N. Takorabet, "Implementation of PD-PI Controller for Boost Converter Using GWO Algorithm," *2022 14th International Conference on Electronics, Computers and Artificial Intelligence (ECAI)*, pp. 1-7, 2022.

[38] L. David, "An Introduction to Observers," *IEEE Transaction on Automatic Control*, vol. AC-16, no. 6, pp. 596-602, 1971.

[39] M. Almawlawe, D. Mitić, D. Antić, and Z. Ić, "An approach to the microcontroller-based realization of boost converter with quasi-sliding mode control," *Journal of Circuits, Systems and Computers*, vol. 26, no. 07, p. 1750106, 2017.

[40] J. A. Solsona, S. G. Jorge, and C. A. Busada, "Nonlinear Control of a Buck Converter Which Feeds a Constant Power Load," *IEEE Transactions on Power Electronics*, vol. 30, no. 12, pp. 7193-7201, 2015.

[41] R. Leyva, L. Martinez-Salamero, H. Valderrama-Blavi, J. Maixe, R. Giral, and F. Guinjoan, "Linear state-feedback control of a boost converter for large-signal stability," *IEEE Transactions on Circuits and Systems I: Fundamental Theory and Applications*, vol. 48, no. 4, pp. 418-424, 2001.

[42] M. L. Kumari, S. Bhattacharya, and U. S. Triar, "Stabilization of boost converter with output filter using LQR based state-feedback controller," *International Conference on Intelligent Systems and Control (ISCO)*, pp. 1-6, 2016.

[43] M. U. Iftikhar, E. Godoy, P. Lefranc, D. Sadarnac, and C. Karimi, "A control strategy to stabilize PWM dc-dc converters with input filters using state-feedback and pole-placement," *IEEE 30th Int. Telecommu nications Energy Conference*, pp. 1-5, 2008.

[44] M. Gheisarnejad, H. Farsizadeh, and M. H. Khooban, "A Novel Nonlinear Deep Reinforcement Learning Controller for DC–DC Power Buck Converters," *IEEE Transactions on Industrial Electronics*, vol. 68, no. 8, pp. 6849-6858, 2021.

[45] N. Swaminathan, N. Lakshminarasamma, and Y. Cao, "DCM and CCM Operation of Buck-Boost Full-Bridge DC-DC Converter," *2021 IEEE Applied Power Electronics Conference and Exposition (APEC)*, pp. 292-297, 2021.

[46] C. O. Omeje, A. O. Salau, and C. U. Eya, "Dynamics analysis of permanent magnet synchronous motor speed control with enhanced state feedback controller using a linear quadratic regulator," *Heliyon*, vol. 10, no. 4, pp. 1-15, 2024.

[47] Z. H. Saleh *et al*., "Enhanced Dynamic Control of Quadcopter PMSMs Using an ILQR-PCC System for Improved Stability and Reduced Torque Ripples," *Journal of Robotics and Control (JRC)*, vol. 5, no. 6, pp. 1652-1663, 2024.

[48] M. -L. Chiu, I. -F. Lo, and T. -H. Lin, "A Time-Domain CCM/DCM Current-Mode Buck Converter with a PI Compensator Incorporating an Infinite Phase Shift Delay Line," *ESSCIRC 2023-IEEE 49th European Solid State Circuits Conference (ESSCIRC)*, pp. 441-444, 2023.

[49] P. Azer and A. Emadi, "Generalized State Space Average Model for Multi-Phase Interleaved Buck, Boost and Buck-Boost DC-DC Converters: Transient, Steady-State and Switching Dynamics," in *IEEE Access*, vol. 8, pp. 77735-77745, 2020.

[50] S.-J. Yoon, N. B. Lai, and K.-H. Kim, "A systematic controller design for a grid-connected inverter with LCL filter using a discrete-time integral state feedback control and state observer," *Energies*, vol. 11, no. 2, p. 437, 2018.

[51] M. H. Rashid, *Power Electronics Handbook: Devices, Circuits and Applications*, Butterworth-heinemann, 2007.

[52] I. K. Mohammed, J. A. Neasham, and B. S. Sharif, "Design and implementation of positioning and control systems for capsule endoscopes," *IET Science, Measurement & Technology*, vol. 14, no. 7, pp. 745-754. 2020.

[53] I. K. Mohammed, A. I. Abdulla, and J. M. Ahmed, "Speed Control of DC Motor Using MRAC and Genetic Algorithm Based PID Controller," *International Journal of Industrial Electronics and Electrical Engineering*, vol. 8, no. 1, pp. 1–6, 2020.

[54] J. Águila-León, C. Palacios, C. Salgado, and E. Perez, "Optimal PID parameters tunning for a DC-DC boost converter: A performance comparative using grey wolf optimizer, particle swarm optimization and genetic algorithms," *Proc. of IEEE Conference on Technologies for Sustainability*, pp. 1–6, 2020.

[55] I. A. Jaddoa, "Integration of Convolutional Neural Networks and Grey Wolf Optimization for Advanced Cybersecurity in IoT

Systems," *Journal of Robotics and Control*, vol. 5, no. 4, pp. 1189-1202, 2024.

[56] G. F. Shidik, "Optimizing Parameters for Earthquake Prediction Using Bi-LSTM and Grey Wolf Optimization on Seismic Data," *Journal of Robotics and Control (JRC)*, vol 5, no. 4, pp. 1117-1127, 2024.

[57] S. Hossient, M. Reza, B. Nicu, T. Phatiphat, and T. Noureddine, "Implementation of PD-PI controller for boost converter using GWO algorithm," *Proc. of International Conference on Electronics, Computers and Artificial Intelligence (ECAI)*, pp. 1–7, 2022.

[58] M. Ghalambaz, R. J. Yengejeh, and A. H. Davami, "Building energy optimization using Grey Wolf Optimizer (GWO)," *Case Studies in Thermal Engineering*, vol. 27, pp. 1-16, 2021.

[59] G. A. Aziz, S. W. Shneen, F. N. Abdullah, and D. H. Shaker, "Advanced optimal GWO-PID controller for DC motor," *International Journal of Advances in Applied Sciences (IJAAS)*, vol. 11, no. 3, pp. 263-276, 2022.

[60] D. G. Luenberger, "An Introduction to Observers," *IEEE Transaction on Automatic Control*, vol. AC-16, no. 6, pp. 596-602, 1971.

[61] M-H, Shin and D-S Hyun, "Speed sensorless stator flux-oriented control of induction machine in the field weakening region," *IEEE Transaction on Power Electronics*, vol. 18, no. 2, pp. 580-586, 2003.

[62] Zs. Horváth and Gy. Molnárka, "Design Luenberger observer for an electromechanical actuator," *Acta Technica Jaurinensis*, vol. 7, no. 4, pp. 328-343, 2014.

[63] J. Lunze, *Regelungstechnik 2*, Springer, pp. 337-366, 2010.

[64] A. Angermann, M. Beuschel, M. Rau, and U. Wolfahrt, "Matlab Simulink Stateflow," *Oldenburg Verlag*, pp. 173-177, 2007.